PHYSICAL REVIEW A **83**, 031801(R) (2011)

Classification of light sources and their interaction with active and passive environments

Ramy G. S. El-Dardiry,* Sanli Faez, and Ad Lagendijk
FOM Institute for Atomic and Molecular Physics AMOLF, Science Park 104, NL-1098 XG Amsterdam, The Netherlands
(Received 13 September 2010; published 8 March 2011)

Emission from a molecular light source depends on its optical and chemical environment. This dependence is different for various sources. We present a general classification in terms of constant-amplitude and constant-power sources. Using this classification, we have described the response to both changes in the local density of states and stimulated emission. The unforeseen consequences of this classification are illustrated for photonic studies by random laser experiments and are in good agreement with our correspondingly developed theory. Our results require a revision of studies on sources in complex media.

DOI: 10.1103/PhysRevA.83.031801 PACS number(s): 42.25.Dd, 32.50.+d, 42.55.Zz

Atomic and molecular light sources are essential tools in the natural sciences. Physicists use these light sources in a great variety of situations, for example, to study light-matter interactions in the context of cavity quantum electrodynamics [1,2], to probe vacuum fluctuations inside and around photonic and plasmonic nanostructures [3,4], or as building blocks for lasers [5]. In the life sciences, fluorescent proteins quickly became one of the most important workhorses soon after their discovery [6]. Major engineering efforts are now devoted to inventing light-source-based microscopy techniques in order to obtain improved resolution and sensitivity [7,8].

The prominence of light sources in scientific experiments requires a well-defined classification of different types of sources. We propose such a classification analogous to the field of electronics, where every circuit design incorporates a well-defined source. In electronics, ideal sources are classified as constant-current sources or constant-voltage sources, depending on their response to a certain load [9].

Mathematically, a point source (sink) is incorporated by a positive (negative) divergence ($S = \nabla \cdot \mathbf{J}$) of a certain vector quantity in space. In order to be classified as a source for light, light should either be created by conversion from a different type of energy, e.g., by electroluminescence, or by a photochemical process in which the absorbed excitation photon differs in frequency from the emitted photon, e.g., in three- and four-level systems. In contrast, two-level systems cannot be considered as light sources; they are scatterers instead. Although we limit ourselves in this manuscript to a discussion of four-level systems, our approach is general and can be applied to other light-generation mechanisms as well.

In a four-level system there are, in general, two decay channels from the lowest vibrational sublevel of the excited state to a vibrational sublevel of the ground state: a radiative channel and a nonradiative channel. These two relaxation mechanisms are competing for the number of molecules in the excited state, similar to the way two parallel resistances are competing for current in a simple electronic circuit. The quantum efficiency of the molecule describes the ratio between the radiative and total decay rate. To qualify for a constant-power source (CPS), the power emitted by the radiative channel must be independent on any change in the "load" of the radiative decay channel. In a constant-amplitude source (CAS) the number of transitions is conserved, but the power emitted by the source is dependent on the conductivity of the radiative decay channel.

In this Rapid Communication, we study the influence of light-source typology on the generation of light in complex media. We provide a clear demonstration of the relevance of our classification with new random laser experiments, where different kinds of light sources act as different gain media. In addition to these new experimental results we provide a description of the interaction of light sources with their environment by calculating the power emitted by a light source in the vicinity of a single scatterer. Our theoretical and experimental studies emphasize that the response of a light source to either stimulated emission or a change in the local density of states (LDOS) depends on its class. In the end, we discuss the impact of CPS and CAS on studies on light sources and multiple scattering.

Experiment. In a random laser [10] the role of sources is twofold: first, they are seeds of spontaneous light emission; second, they amplify light by stimulated emission of radiation. Due to the multiple-scattering feedback mechanism, random lasers form a unique laser system. In contrast to conventional lasers, they have a statistically isotropic mode selectivity, as illustrated by the cartoons in Figs. 1(a) and 1(b). The mode selection is solely determined by the spectral shape of the gain curve. In a random laser, measuring the emitted energy into a large enough solid angle corresponds to measuring the total emitted intensity: diffusion mimics an integrating sphere. In our experiments, we utilize this much-neglected property of random lasers to study the energy emitted by light sources with different quantum efficiencies for varying pump rates.

Three molecular light sources were studied in a random laser configuration by suspending titania particles (R900 DuPont, volume fraction 1%) into three different 1-mM solutions of organic dyes in methanol. The three dye solutions acted as gain media and were chosen on the basis of their quantum yields ϕ reported in the literature [11,12]: Rhodamine 640 P ($\phi = 1$), Cresyl Violet ($\phi = 0.54$), and Nile Blue ($\phi = 0.27$); see Methods in the Supplemental Material [13] for more information on the used optical setup and the sample preparation.

For all random laser samples, the fluorescent emission spectra were recorded for different values of the pump fluence below and above threshold. In Fig. 1(c), emission spectra

*dardiry@amolf.nl; http://www.randomlasers.com

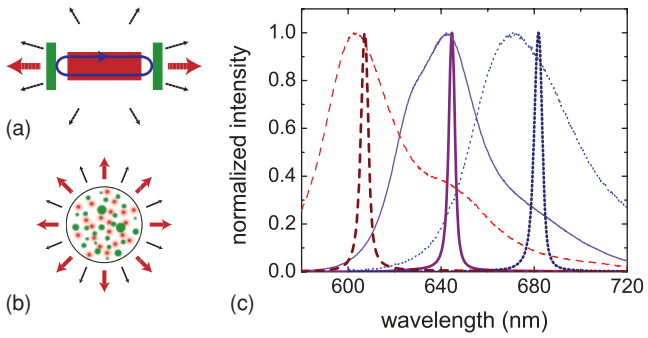

FIG. 1. (Color) Illustration of emission directionality below threshold (black arrows) and above threshold (thick red arrows) in (a) a conventional laser and (b) a random laser. In a random laser the emitted light by an ensemble of sources is always omnidirectional. (c) Experimental emission spectra below and narrowed spectra above random laser threshold for three different light sources: Rhodamine 640 P (red dashed lines), Cresyl Violet (purple solid lines), and Nile Blue (blue dotted lines). The β factor is determined by the quotient of the area of the normalized spectra above and below threshold.

far below and far above threshold are plotted. The spectra above threshold are narrower by a factor ~10 compared to the spectra below threshold, and the peaks are slightly red shifted due to reabsorption. Figure 2 shows the peak [Figs. 2(a) and 2(b)] and the integrated spectral radiance [Figs. 2(c) and 2(d)] versus the excitation power. The peak spectral radiance shows a clear threshold for all the three random laser systems. In a conventional laser, angular redistribution of light emission causes a threshold in the spectrally integrated power of the output beam irrespective of the chosen gain medium. However, in the experimental results shown in Figs. 2(c) and 2(d) we observe that for the random laser with the highest quantum

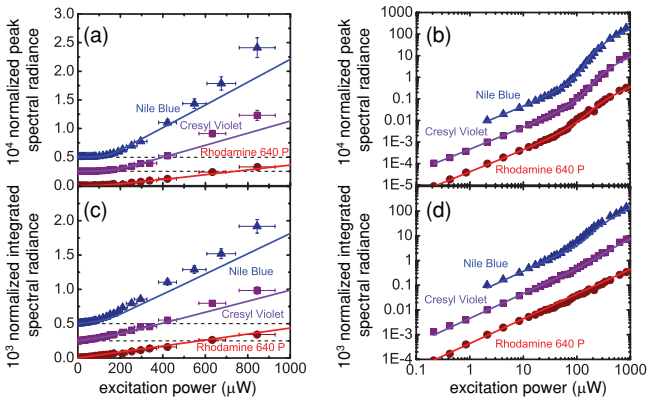

FIG. 2. (Color) Input-output diagrams for random lasers consisting of light sources with low and high quantum efficiencies. Peak spectral radiance versus pump power for three random lasers with different molecular light sources on (a) a linear and (b) a log-log scale. The solid lines are fits to the experimental data. Integrated spectral radiance versus pump power for three random lasers on (c) a linear and (d) a log-log scale. The solid lines are theoretical calculations. The Rhodamine 640 P random laser does not show a clear threshold. All data points in (a)–(d) were normalized to the values at 2.1 μW, and the results for the Nile Blue and Cresyl Violet random lasers were shifted vertically for clarity.

efficiency gain medium (Rhodamine) such a threshold in the integrated spectral radiance is absent.

Random laser model. Standard lasers are described with rate equations [11] describing the number of photons in the cavity mode $q(t)$ and the number of molecules in the upper laser level $N(t)$. For a four-level system it is usually assumed that only the population of the ground state and the upper-laser level are significant. To model our random laser experiment, we extend such a set of equations with an equation describing the number of photons $w(t)$ emitted outside the lasing mode:

$$\frac{dq}{dt} = -q\gamma_c + \beta\gamma_r Nq + \beta\gamma_r N, \tag{1}$$

$$\frac{dw}{dt} = -w\gamma_c + N\gamma_r(1-\beta), \tag{2}$$

$$\frac{dN}{dt} = R - N\gamma_{tot} - \beta\gamma_r Nq. \tag{3}$$

Here R is the pump photon rate, γ_c is the cavity decay rate, and γ_{tot} is the total decay rate, with $\gamma_{tot} = \gamma_r + \gamma_{nr}$, where γ_r and γ_{nr} are the radiative and nonradiative decay rates, respectively. The spontaneous emission factor β describes what fraction of the spectrum contributes to the lasing emission [14]. Due to the absence of angular mode selection in a random laser, the β factor suffices for distinguishing photons inside and outside the lasing mode: for photons emitted in the wings of the spectrum, stimulated emission is neglected in rate equation (2), whereas for photons emitted into the peak of the spectrum, Eq. (1), stimulated emission is added to the spontaneous emission rate. The random lasers considered here have a smooth spectrum above threshold. The particular case of a random laser with spectral spikes [15] requires a different formulation [5]. We determine the β factor for the three random lasers by calculating the ratio of the integrated spectra above and below threshold after normalizing to the peak value [14]: for Rhodamine $\beta = 0.099$, for Cresyl Violet $\beta = 0.088$, and for Nile Blue $\beta = 0.076$.

To infer the threshold, the steady-state solutions to Eqs. (1)–(3) for the number of photons in the peak and the wings of the spectrum are calculated:

$$q = -\frac{1}{2\beta\phi} + \frac{R}{2\gamma_c} + \frac{1}{2}\sqrt{\left(\frac{1}{\beta\phi} - \frac{R}{\gamma_c}\right)^2 + 4\frac{R}{\gamma_c}}, \tag{4}$$

$$w = \left(\frac{R}{\gamma_c} - q\right)\frac{1-\beta}{\phi^{-1}-\beta}. \tag{5}$$

Above threshold the slope of the solution for q changes, and the β factor and ϕ determine the "smoothness" of the transition. Obtained analytical expressions for the threshold for the peak and integrated spectral radiance are

$$R_{th}^{peak} = [(\beta\phi)^{-1} - 1]\gamma_c, \tag{6}$$

$$R_{th}^{int} = [(\beta\phi)^{-1} - \beta^{-1}]\gamma_c. \tag{7}$$

Thus, it is incorrect practice to use R_{th}^{int} to find the threshold of a random laser because $R_{th}^{int} \to 0$ when $\phi \to 1$.

A fit of the experimental peak spectral radiance with Eq. (4) gives ϕ and R/γ_c. This second fit parameter scales the power axis. A third fit parameter scaled the y axis. These fits are shown in Figs. 2(a) and 2(b) and yielded the following values for the quantum efficiency: Rhodamine $\phi = 1 \pm 0.09$, Cresyl

Violet $\phi = 0.57 \pm 0.04$, and Nile Blue $\phi = 0.25 \pm 0.02$. A systematic deviation might be caused by the method used for estimating the β factor [14]. A single random laser experiment thus suffices for analyzing the quantum efficiency of a light source in a complex medium. Using Eq. (5) and the measured values for β and ϕ, we can make a theoretical prediction for the integrated spectral radiance versus excitation power. These theoretical curves are plotted in Figs. 2(c) and 2(d) and are in great agreement with the experimental data.

The remarkable observation of a different behavior of the integrated spectral radiance, that is, the total emitted power, for the three random lasers as a function of input power is well explained by the concept of CPS and CAS. The random laser threshold indicates the transition from spontaneous emission to stimulated emission as the main mechanism of radiation. In the case of a gain medium consisting of sources with near-unity quantum efficiency, this transition does not influence the ratio between the number of excitation photons that are absorbed and the number of photons that are emitted: the total emitted power scales linearly with the total absorbed power. Hence, we classify these high-quantum-efficiency dye molecules as CPS for light. The threshold in the peak spectral radiance simply indicates the energy is spectrally redistributed from the wings to the peak of the spectrum. For a gain medium consisting of sources with a low quantum efficiency, the transition from spontaneous emission to stimulated emission also changes the ratio between the nonradiative and the radiative decay channel. The number of transitions is conserved, but the load of the radiative decay channel is decreased, causing the total emitted power to scale nonlinearly with the pump power. Low-quantum-efficiency molecules should be classified as CAS for light, as will be discussed in the following paragraphs.

A single scatterer and a source. We just showed how invoking stimulated emission of radiation changes the "resistance" of an optical transition; alternatively, one can change the LDOS at the position of the source. Let us start by analyzing the output power of a widely used classical dipole source and then introduce a generalized expression for a source based on a rate equation analysis. For a point source,

$$j(\mathbf{r},t) = j_0 \delta(\mathbf{r} - \mathbf{r_0}) \exp(-i\omega t) + \text{c.c.}, \tag{8}$$

the output power is related to the LDOS. Figure 3 is a schematic representation of the Green function G describing propagation to $\mathbf{r}$ from a unit source ($j_0 = 1$) located at $\mathbf{r_0}$ in presence of a scatterer at $\mathbf{R_s}$. In a homogeneous background, this Green function is given by

$$G_\omega(\mathbf{r},\mathbf{r_0}) = G^0_\omega(\mathbf{r} - \mathbf{r_0}) + G^0_\omega(\mathbf{r} - \mathbf{R_s}) t(\omega) G^0_\omega(\mathbf{R_s} - \mathbf{r_0}). \tag{9}$$

Here G^0_ω is the free space Green function, and $t(\omega)$ is the t matrix of the scatterer. To find the power P_{src} radiated by the

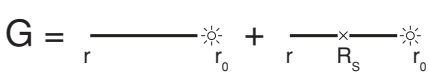

FIG. 3. Diagram of a Green function describing propagation from a constant-amplitude source at $\mathbf{r_0}$ to $\mathbf{r}$ with one possible scattering event at $\mathbf{R}_s$.

source in Eq. (8), we integrate the divergence of the current for an infinitesimally small volume around the source and find

$$P^{\text{CAS}}_{\text{src}} / P_0 = -\frac{4\pi c}{\omega} \text{Im} G_\omega(\mathbf{r_0},\mathbf{r_0}) \equiv \frac{4\pi^2 c^3}{\omega^2} \rho(\mathbf{r_0},\omega), \tag{10}$$

where P_0 is the emitted power without the scatterer present and ρ is the LDOS. The final step is only valid for absorption-free environments. We prefer to phrase our discussion in terms of LDOS, but the reader should note that external absorption can easily be included by replacing the LDOS with $-\frac{\omega}{\pi c^2}\text{Im}G_\omega$.

The emitted power is thus dependent on the LDOS, which acts as the inverse of a load on the source. Since the emitted power can be both higher and lower compared to the vacuum situation, the source we introduced in Eq. (8) is clearly not a CPS; rather, we classify it as a CAS originating from the constant amplitude in Eq. (8). However, from a steady-state rate equation analysis, which is explained in full for the interested reader in the Supplemental Material, we derive that the photon production rate for a source with nonradiative and radiative decay channels is proportional to $\gamma_{\text{r}} \frac{\gamma_{\text{e}}}{\gamma_{\text{r}} + \gamma_{\text{nr}}}$, where γ_{e} is the excitation rate. We assume the excitation rate to be constant and independent from the environment. Our analysis can easily be extended, however, for environment-dependent excitation rates. Therefore, the emitted power reads

$$P_{\text{src}} / P_0 = \frac{\gamma_{\text{r}}}{\gamma_{\text{r}} + \gamma_{\text{nr}}} \Big/ \frac{\gamma^{(0)}_{\text{r}}}{\gamma^{(0)}_{\text{r}} + \gamma_{\text{nr}}} = \frac{4\pi^2 c^3}{\omega^2} \rho(\mathbf{r_0},\omega) \frac{\gamma^{(0)}_{\text{r}} + \gamma_{\text{nr}}}{\gamma_{\text{r}} + \gamma_{\text{nr}}}, \tag{11}$$

where in the final expression we have replaced the radiative decay rate with the LDOS using Fermi's golden rule, which states that in nonabsorbing media $\gamma_{\text{r}} = A\rho$, with A defined as an atomic factor. From this equation it becomes clear that Eq. (8) should be adjusted in a similar way:

$$j(\mathbf{r},t) = \sqrt{\frac{\gamma_{\text{e}}}{\gamma_{\text{r}} + \gamma_{\text{nr}}}} \delta(\mathbf{r} - \mathbf{r_0}) \exp(-i\omega t) + \text{c.c.} \tag{12}$$

In deriving this expression, we implicitly make the generally valid assumption that atomic coherence decays very fast. From Eq. (12) we deduce that the axiomatic expression (8) only applies to a four-level source when $\gamma_{\text{nr}} \gg \gamma_{\text{r}}$, a situation often avoided in experiments. If this condition is not fulfilled, for instance, in the case of a CPS, the strength of the source depends explicitly on the radiative decay rate and therefore the LDOS. This dependence of power on the environment is valid for any complex system.

To find the correct wave function from a single source or collection of sources,

$$\psi(\mathbf{r}) = \int G_\omega(\mathbf{r},\mathbf{r_0}) j\{G_\omega(\mathbf{r_0},\mathbf{r_0})\} \, d\mathbf{r_0} \tag{13}$$

then becomes very involved since it requires knowledge of the Green function for both the propagation and the generation of light. Although this dramatically hinders analytic calculations, it should be straightforward to correctly adjust the source strength in numerical calculations. Introducing stimulated emission into our analysis and eventually into Eq. (12) leads

to an increase of the radiative decay rate. This increase leaves a CPS unaltered, but a CAS will start to look more like a CPS. Stimulated emission and the LDOS can thus be used to engineer light sources with γ_r/γ_{nr} as a control parameter.

Conclusion and discussion. We have developed a classification scheme for light sources. Sources with unit quantum efficiency are classified as constant-power sources for light, and those with a low quantum efficiency are classified as constant-amplitude sources. We demonstrated that this classification directly influences the interpretation of photonic experiments. In the case of a CAS, both stimulated emission and changes in the LDOS alter the load of the radiative transition and thereby the output power.

Our classification of light sources is applicable to all photonic systems. In random media, recently predicted infinite range correlations are caused by an interaction between a light source and a nearby scatterer [16]. Since for a classical dipole source this C_0 correlation is equivalent to fluctuations in the LDOS [17,18], it is very likely that a CPS will yield different results. We hope our work encourages the use of more well-defined sources in theory and will help in choosing the right type of source for the desired measurement.

Note added. Recently, a theoretical paper by Greffet *et al.* [19] was published where a similar concept was developed, emphasizing electronic circuit analogies in the field of nanoantennas.

Acknowledgments. We thank Allard Mosk and Willem Vos for stimulating discussions. Timmo van der Beek is acknowledged for help with the sample preparation. This work is part of the research program of the 'Stichting voor Fundamenteel Onderzoek der Materie (FOM), which is financially supported by the Nederlandse Organisatie voor Wetenschappelijk Onderzoek (NWO).

[1] T. Wilk, S. C. Webster, A. Kuhn, and G. Rempe, Science **317**, 488 (2007).
[2] L. Sapienza, H. Thyrrestrup, S. Stobbe, P. D. Garcia, S. Smolka, and P. Lodahl, Science **327**, 1352 (2010).
[3] A. F. Koenderink, L. Bechger, H. P. Schriemer, A. Lagendijk, and W. L. Vos, Phys. Rev. Lett. **88**, 143903 (2002).
[4] J. N. Farahani, D. W. Pohl, H. J. Eisler, and B. Hecht, Phys. Rev. Lett. **95**, 017402 (2005).
[5] H. E. Türeci, L. Ge, S. Rotter, and A. D. Stone, Science **320**, 643 (2008).
[6] R. Y. Tsien, Annu. Rev. Biochem. **67**, 509 (1998).
[7] V. Westphal and S. W. Hell, Phys. Rev. Lett. **94**, 143903 (2005).
[8] W. Min, S. Lu, S. Chong, R. Roy, G. Holtom, and X. S. Xie, Nature (London) **461**, 1105 (2009).
[9] P. Horowitz and W. Hill, *The Art of Electronics* (Cambridge University Press, New York, 1989).
[10] D. S. Wiersma, Nat. Phys. **4**, 359 (2008).
[11] A. Siegman, *Lasers* (University Science Books, Sausalito, California, 1986).
[12] S. J. Isak and E. M. Eyring, J. Phys. Chem. **96**, 1738 (1992).
[13] See supplemental material at [http://link.aps.org/supplemental/10.1103/PhysRevA.83.031801] for more information on the used optical setup and the sample preparation.
[14] G. van Soest and A. Lagendijk, Phys. Rev. E **65**, 047601 (2002).
[15] H. Cao, Y. G. Zhao, S. T. Ho, E. W. Seelig, Q. H. Wang, and R. P. H. Chang, Phys. Rev. Lett. **82**, 2278 (1999).
[16] B. Shapiro, Phys. Rev. Lett. **83**, 4733 (1999).
[17] B. A. van Tiggelen and S. E. Skipetrov, Phys. Rev. E **73**, 045601 (2006).
[18] A. Cazé, R. Pierrat, and R. Carminati, Phys. Rev. A **82**, 043823 (2010).
[19] J. J. Greffet, M. Laroche, and F. Marquier, Phys. Rev. Lett. **105**, 117701 (2010).